

RESEARCH ARTICLE OPEN ACCESS

Riparian Soils Inform Dissolved Organic Matter Delivery in a Norwegian Subarctic River

Marc Stutter^{1,2}  | Leah Jackson-Blake³ | Maeve McGovern⁴ | Juliana D'Andrilli⁵ | James R. Junker⁵ | Peter Dörsch⁶ | Helen Watson¹ | Stein Rune Karlsen⁷ | Benoît O. L. Demars⁸

¹The James Hutton Institute, Aberdeen, UK | ²Lancaster Environment Centre, Lancaster University, Lancaster, UK | ³Norwegian Institute for Water Research (NIVA), Grimstad, Norway | ⁴Norwegian Institute for Water Research (NIVA), Tromso, Norway | ⁵Dept of Biological Sciences and the Advanced Environmental Research Institute, University of Texas, Denton, Texas, USA | ⁶Norwegian University of Life Sciences, Ås, Norway | ⁷NORCE Norwegian Research Centre AS, Tromsø, Norway | ⁸Norwegian Institute for Water Research (NIVA), Oslo, Norway

Correspondence: Marc Stutter (marc.stutter@hutton.ac.uk)

Received: 25 April 2025 | **Revised:** 1 August 2025 | **Accepted:** 15 August 2025

Funding: This work was supported by the Norwegian Research Council FRIPRO project QUANTOM (314957).

Keywords: dissolved organic matter cycling | landscape processes | nitrogen | phosphorus | riparian soils | subarctic carbon

ABSTRACT

Critical factors in dissolved organic matter (DOM) cycling are changing in subarctic to arctic systems, with less knowledge than boreal and temperate systems on soils, flowpaths, and biogeochemistry to inform process understanding and catchment modelling. We test the hypothesis that riparian soils accumulate appreciable concentrations of total and labile carbon (C), nitrogen (N), and phosphorus (P) and contribute strongly to subarctic macronutrient cycling across the terrestrial-to-aquatic interface. Such subarctic soils are rarely described, especially in terms of combining C, N, and P data together. We sampled hillslope to riparian transitions at four subcatchments (31–61 km²) of the 16,000 km² Norwegian River Tana (69°N) to: (i) assess soil C, N, and P concentrations, stocks, soil reactive chemistry, and water soluble macronutrient forms; (ii) understand spatial variability; (iii) consider the role of near-channel soils in DOM fate across scales in large subarctic rivers, including experimentation on subsoil DOM sorption and soil flowpath conceptualisation. Horizon-based differences in total C, N, P concentrations and water-extracted macronutrients showed wetter riparian and stream-side positions had enhanced total C, N concentrations and DOC concentrations (up to ~200 mgC/L). Stocks of C (2–28 kg/m²), N (0.1–1.2 kg/m²), and P (<0.1–0.9 kgP/m²) were highly variable, greatest in riparian positions in the plateau tundra sites. Similar P stocks to that of N suggest moderate P and low N supply to ecosystems. Organo-mineral soil transitions studied show lateral flows through high DOM source layers near-channel and important hillslope interactions between surface and subsoil pathways capable of retaining (30% DOC removal in column experiments) and altering DOM quality. Our data inform frameworks for DOM cycling in large arctic riverscapes, by: (i) showing strong DOM sources in near-channel soils highly connected to headwaters, (ii) understanding amounts and quality (absorbance properties and stoichiometry) of potentially transported DOM, and (iii) reactivity and flow routing controlling DOM mobility, sorption and alteration of DOM forms. There is a clear role for combining soil biogeochemistry and hydrology to look inside the catchment ‘box’ to better understand DOM cycling in changing ecosystems.

1 | Introduction

Soil organic matter (SOM) is a dominant source of dissolved organic matter (DOM) to rivers in semi-natural catchments.

Globally, gradients of precipitation and temperature have led to considerable SOM reserves in mid to higher latitudes. Despite a considerable body of literature on how soils control DOM exports in temperate to boreal catchments (Jansen et al. 2014),

This is an open access article under the terms of the [Creative Commons Attribution](#) License, which permits use, distribution and reproduction in any medium, provided the original work is properly cited.

© 2025 The Author(s). *European Journal of Soil Science* published by John Wiley & Sons Ltd on behalf of British Society of Soil Science.

Summary

- Subarctic ecosystems are change sensitive and have a key role in global nutrient cycling.
- Soil knowledge is needed to support dissolved organic matter (OM) cycling modelling.
- Subarctic riparian soils have enhanced OM stocks and biogeochemical reactivity.
- Landscape complexity in soil chemistry and flow-paths needs to be represented in catchment models.

recent focus has been brought to DOM delivery and reactivity along the soil-freshwater-sea continuum in arctic and subarctic catchments (Prowse et al. 2015). This is due to increased sensitivity to climate and other superimposed environmental changes at higher latitudes and the role this may collectively have in influencing large-scale global nutrient cycles (Shogren et al. 2019; Frey et al. 2007). In particular, SOM stocks, compositions, and biogeochemical interactions in high latitude catchments are poorly understood as a basis for incorporating large northern rivers into modelling of future nutrient cycle changes (Wieder et al. 2019).

Soil surveys have historically addressed the need for classification and management of soils in agricultural regions. Ecosystems at higher latitudes generally have much less developed soil resources and knowledge relative to lower latitudes (Batjes 2002), but this is spatially variable. Canada has a unified national soil profile database with dense coverage at lower latitudes, extending well into high latitudes (NSDB 2022). In contrast, soil mapping in Norway is limited to agricultural lowlands (Arnoldussen 1999) and broader coverage is lacking such that Norway has been excluded from some European soil carbon (C) mapping due to data paucity (de Brogniez et al. 2015) and the potential uncertainties when extrapolating from few samples to national habitat scales (Bartlett et al. 2020). In some cases, soil types are assumed through broader habitat and land cover mapping, informed by remote sensing. Whilst this can help classify broad soil classes, for example, peat, organo-mineral, and mineral soils, important detail on spatial organisation, heterogeneity, and soils of disproportionate influence are overlooked. Given these uncertainties and the rapid environmental changes at higher latitudes, concerted effort is being given to increase observations of sensitive soils and to document the effects on Arctic ecosystem processes (Kjær et al. 2024; Miner et al. 2021; Mueller et al. 2015).

An important step to integrate soil into catchment hydrochemical and biogeochemical process research is the linking of soil functional types and landscape positions to source and transport controls on river solute and particulate fluxes (Shogren et al. 2019; Abril and Borges 2019). From broader whole catchment predictors like percent catchment cover of peaty soils relating to river DOM fluxes across landscape types (Aitkenhead et al. 1999), research targets have shifted towards hot spots and hot moments, encompassing new soils knowledge (Krause et al. 2017). Spatial organisation and resulting connectivity of soils in catchments is important to solute delivery and reactivity (Abril and

Borges 2019; Covino 2017; Laudon and Sponseller 2018) as well as ecology (Broll et al. 2007). Riparian soils have a disproportionate effect on matter fluxes and altered processes sensitivity because of their landscape position within the drainage network, specific soil type dominance, and change susceptibility (Stutter et al. 2023; Zhang and Furman 2021). Responsive riparian zones are known to strongly influence dissolved organic carbon (DOC) loads and compositions in temperate and boreal climates, and in the Arctic (Harms and Ludwig 2016). In boreal forest regions, spatio-temporal delivery concepts of DRIPS (discrete riparian inputs) and Dominant Source Layers (near surface layers of disproportionately large water-soluble DOM concentrations) have been developed to model DOM exports with 2D and 3D soil wetting and flushing (Ploum et al. 2021). In advancing this understanding, classification schemes of soil water flow path behaviours in relation to soil types (Scheider et al. 2007) and other geomorphic units for assessing nutrient stocks (Ola et al. 2022) are useful if available at appropriate scales.

The subarctic occupies the intermediate zone between arctic frozen soils and the more widely studied boreal-temperate peat and organo-mineral soil ecosystems. A particular seasonality affects hydrology and biogeochemistry associated with low overall rainfall, periods of frozen dormancy, strong flushing during spring snow melt, and then biologically active summer periods dominated by low river flows. Hence, soils have distinct connectivity behaviours of catchment areas to the drainage networks in space and time. During the freshet (snowmelt flood) a high degree of hydrological connectivity occurs across large catchment areas and solute source zones are maximised. This flood pulse is short-lived and its contribution towards overall annual DOM quality and fluxes is generally poorly quantified. Conversely, low flow conditions constrain connectivity of outlying areas and increase the importance of valley bottom and wetland DOM contributions. With general low rainfall, the impacts of occasional rain-driven flushing events to network DOM dynamics and the properties and relevance of contributing catchment 'hot-spots' are not well studied (Shogren et al. 2019).

The current study was part of a wider project, QUANTOM (QUANTification of dissolved Organic Matter and the metabolic balance in river networks; 2021–2025) improving understanding of DOM sources and delivery along the River Tana and in-river transformations leading to carbon dioxide (CO_2) emissions. To support this, we set out to test the hypothesis that due to their watershed position and hydrologic connectivity, near-channel riparian soils accumulate appreciable concentrations of total and labile C, nitrogen (N), and phosphorus (P) and, therefore, may have strong contributions to macronutrient cycling across the terrestrial-to-aquatic interface. More specifically, we first assess (i) concentrations and stocks of soil carbon (C), nitrogen (N), and phosphorus (P) macronutrients (total and water extractable), (ii) geochemical properties, and (iii) translate soil profiles into soil-type hydrology in seldom-characterised subarctic riparian soils. Second, we (i) test whether soil nutrient concentration, stocks, and geochemical properties relating to retention versus mobilisation in soils differ more within profiles, along transects (near channel to base of the hill slope) or between subcatchments draining different vegetation types. Third, we test sorption and then desorption of native topsoil DOM by subsoil material rich

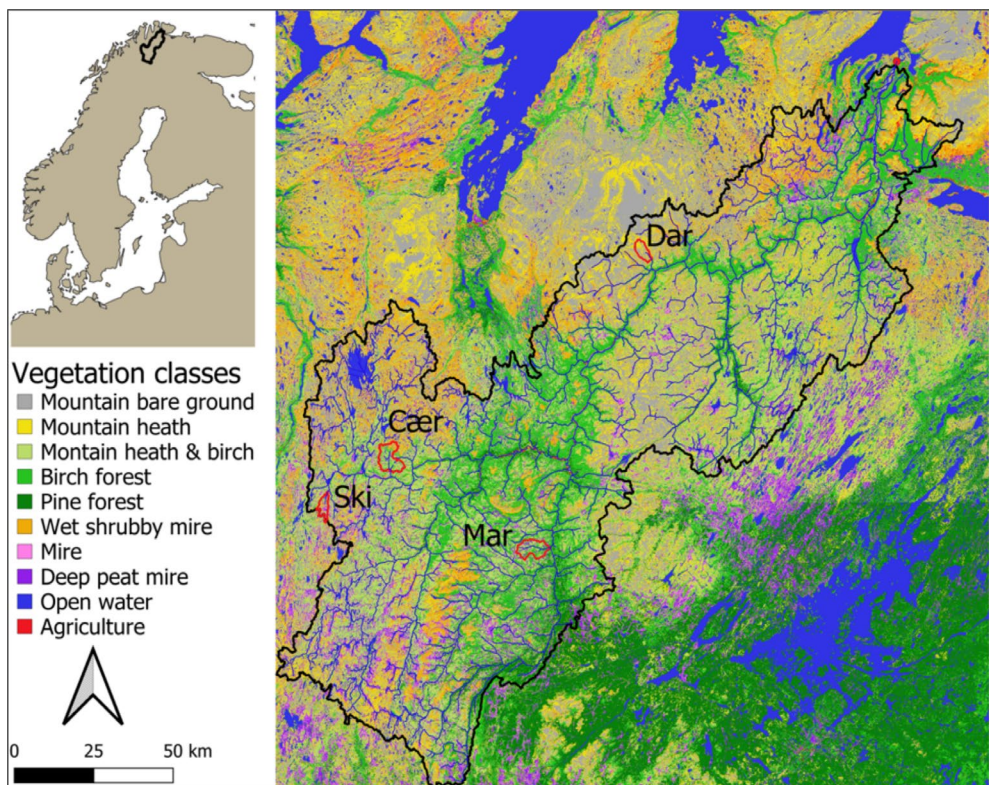


FIGURE 1 | Vegetation and location map of the subarctic River Tana basin, northern Norway, draining to the Barents Sea (Arctic Ocean). The four subcatchments are delineated in red and include: Cærrogæsjohka (Cær), Mareveadji (Mar), Skierrejohka (Ski) and Darjohka (Dar). The river outlet is notified with a red dot (North-East). The channel network is derived from Copernicus 30 m global DEM (European Space Agency 2024) using Q-GIS (QGIS Development Team 2024).

in sesquioxide in a soil column experiment. Finally, we consider how the resulting knowledge of near-channel soil processes helps inform river biogeochemical study of DOM origins and fate across scales in large subarctic rivers.

2 | Methods

2.1 | River Tana Catchment and Selected Sites

The continuum under wider study was the 16,380 km² River Tana catchment in northern Norway (Figure 1), with four subcatchments for the present study selected amongst monitored basins spanning representative vegetation zones and presumed different soils (details below). We did not include deep peat mire and palsas (discontinuous permafrost) recently surveyed (Kjær et al. 2024). Note the surface area of palsas in Tana is extremely limited and not necessarily adjacent to the stream network.

Located north of the Arctic Circle, the River Tana has a subpolar climate with limited seasonal variation in precipitation, long winters and short summers. With a low population density (<0.5 persons/km²), it has limited human impacts apart from those related to reindeer herding and grazing, and some grass production along the lower reach of the main stem. Amongst the Norwegian routinely monitored waterbodies, the rivers in the region are characterised by low N and P concentrations and good water quality (Kaste et al. 2024). The four subcatchments outlets had average concentration ranges of 1.1–9.6 mgC/L for dissolved organic

carbon, 0.11–0.19 mgN/L total dissolved N and <0.005 mgP/L for total dissolved P in 2022 (Table 1).

In the absence of mapped soils, we created a vegetation map and used it to select subcatchment areas. The vegetation map was based on Sentinel-2 satellite data with 10 m pixel resolution (Drusch et al. 2012). We merged 10 cloud-free tiles and classified them using K-means clustering. The classified map was interpreted in the field and cross-referenced with previous vegetation maps (Johansen and Karlsen 2005; Karlsen et al. 2017, 2023). The final vegetation map had 23 classes. Figure 1 presents an aggregated version with 10 vegetation classes.

As part of the wider project, tracer studies were performed to characterise lateral flows. The four subcatchments (Table 1) were 31–64 km², a spatial scale where streams are strongly connected to the land with substantial lateral and/or vertical flow exchanges (Table 1). Dominant habitats included lichen birch forest, mountain heath, mire, snow-bed, and boulder (Table 1; Figure 1).

2.2 | Soil Sampling and Field Characterisation

Soils were sampled once in October 2022 at four locations, one each in the four subcatchments: Cærrogæsjohka (Cær), Mareveadji (Mar), Skierrejohka (Ski), Darjohka (Dar) (Table 1, Figure 1). Target sampling points were selected by analysing aerial images and walk-over surveys to confirm

TABLE 1 | Attributes of the four studied sites in the River Tana watershed.

Attributes	Cær	Mar	Ski	Dar
Place name	Cærrogæsjohka	Mareveadji	Skierrejohka	Darijanka
Latitude, Longitude	69.3914, 24.4745	69.2009, 25.6820	69.3279, 24.0108	69.9695, 26.4191
Elevation (m a.s.l.)	291	164	357	280
Catchment area (km^2)	49	38	64	31
Mean catchment elevation (m) ^a	387	282	432	539
Mean rain 2022 (mm) ^a	535	465	533	545
Mean temp 2022 ($^{\circ}\text{C}$) ^a	-0.9	0.0	-1.0	-0.9
Proportion of lateral inflows in two stream segments ^b	20% and -37%	14% and -8%	8% and 0%	13% and 11%
Terrain form	Hummocky stream bank, straight slope (2° – 5°), remnant channels, then concave base of gentle hillslope	Straight slope to stream bank (2° – 5°), then abrupt change to moderate (12° – 15°) hillslope	Hummocky flat, then straight slope (5° – 8°) with remnant channels, to base of 45° hillslope	Hummocky, rocky, braided active channel, then straight slope (5° – 8°) and boulder, to 45° hillslope
Sampled soil positions	Lower ($n=3$), mid ($n=3$), upper ($n=3$)	Lower ($n=3$), upper ($n=3$)	Lower ($n=3$), mid ($n=3$), upper ($n=3$)	Lower ($n=3$), mid ($n=3$), upper ($n=3$)
Upper and lower transect distance	25 m	10 m	30 m	25 m
Dominant vegetation classes ^c (% of catchment) ^a	MLBF (50%), CBBF (18%), Mire (10%), MHW (8%)	MLBF (48%), CBBF (34%), Mire (14%)	MLBF (40%), Mire (22%), ERGLH (13%), LHHG (10%)	ERGLH (35%), MALSB (20%), LHHG (12%), BB (10%)
Main soil types (WRB major soil types)	Fluvisol (lower) Gleysoil (mid) Podzol (upper)	Fluvisol (lower) Regosol (upper)	Fluvisol (lower) Regosol (mid) Podzol (upper)	Podzol (lower) Regosol (mid) Regosol (upper)
Mean stream flow during spring flood and summer ^c , 2022 ($\text{m}^3/\text{km}^2/\text{day}$) ^a	5739	6241	7331	11,581
	718	619	990	718

(Continues)

TABLE 1 | (Continued)

Attributes	Cær	Mar	Ski	Dar
Mean (range) DOC concentrations ^d , 2022 (mgC/L)	7.9 (4.5–13.9)	9.5 (5.2–18.1)	6.3 (4.2–12.2)	1.1 (0.9–2.2)
Mean DOC flux during spring flood and summer ^c , 2022 (kgC/km ² /day)	43 10	58 7	24 12	14 3

Abbreviations: BB, Bedrock and boulder fields; CBBF, Crowberry–bilberry birch forest; ERGLH, Exposed ridges and heavily grazed lichen heath; LHHR, Lichen heath and heather ridge communities; MALSB, mid alpine and late snow beds; MHW, Meadow, heaths and willow thickets; MLBF, Mountain and lichen birch forest.

^aData taken from Cransac (2023).

^bDetermined the week before the soil profile work from in-stream NaCl tracer studies along two consecutive stream segments (90–294 m long each) contiguous to the soil profiles. Negative percentages indicate net outflows (i.e., net loss of water flow within the reach).

^cSpring flood (May–20 June) and summer (21 June–October).

^dDerived from cDOM sensors and grab samples.

suitable gradients of riparian to hillslope soils. Sample points were perpendicular to the stream channel by 10 to 30 m and 20 to 30 m parallel along the watercourse. Layout followed the idealised conceptual riparian to hillslope gradient depicted in Figure 2. Sampling design comprised three landscape positions: streamside (~1 m from the bank; hereby termed lower), mid (termed mid), and base of hillslope (termed upper) locations (Figure 2), each having a row of three sampled soil profiles. The exception was Mareveadji (Mar) where the short distance (~10 m) to the hillslope led to excluding the mid sampling points. Landscapes of the four locations are shown in Figure 3.

At nine points per location (six at Mar) soil pits (~0.5 m²) were dug with a spade to a maximum achievable depth (~0.4–0.7 m). Site plots and soils were described in terms of slope and local topography, horizon type, depth, colour, texture, stone and root contents, and moisture and other morphological features, and photographed. Vegetation was photographed and described. Samples for chemical analysis ($n=136$) were taken using a trowel from the undisturbed upslope face of the pit at a midpoint of the soil horizons, or multiple samples every ~10 cm for deeper horizons. Samples for soil bulk density were collected using a stainless-steel ring corer (6 cm diameter, 6 cm depth) minimising soil compression. The litter layer was also sampled. Spongy litter layers and rocky horizons could not be sampled for bulk density ($n=51$) and their bulk densities were modelled (Section 2.6; Figure S1). For several horizons where drainage and red colour indicated high subsoil iron (Fe) and aluminium (Al) sesquioxide concentrations, bulk (~1 kg) samples were also taken. Soils were kept field moist at ambient conditions in the field (~2°C–5°C) for a maximum of 5 days, were briefly in transit to two laboratories in Norway and the UK, then kept at 5°C in the dark.

2.3 | Soil Physical Characterisation

Soil core samples (field-moist state) were weighed, then air-dried (30°C, until stable mass, 3–7 days), passed through a 2 mm aperture sieve and reweighed. Stones and woody debris > 2 mm were discarded, but partly decomposed litter was gently pressed through the sieve. This allowed the calculation of the following: air-dried total mass, stone and woody debris-free air-dried mass, percent moisture content, percent stone and woody mass content, and dry bulk density of both total soil and of stone and woody debris-free soil.

2.4 | Soil Chemical Characterisation

Soils for chemical analysis were < 2 mm sieved and air dried. Total C and N were determined on ball-milled subsamples (~2 mg) by combustion analysis with natural abundance stable isotope C and N analysis (Flash EA 1112 CN, Thermo-Finnigan, Italy). The $\delta^{13}\text{C}$ and $\delta^{15}\text{N}$ values were reported in units of per mille (‰) with respect to the international reference material for carbon (Vienna Pee Dee Belemnite; VPDB) and atmospheric air for nitrogen. The presence of inorganic C was determined on a subset ($n=5$) by reanalysis following exposure to fuming concentrated hydrochloric acid (12 M

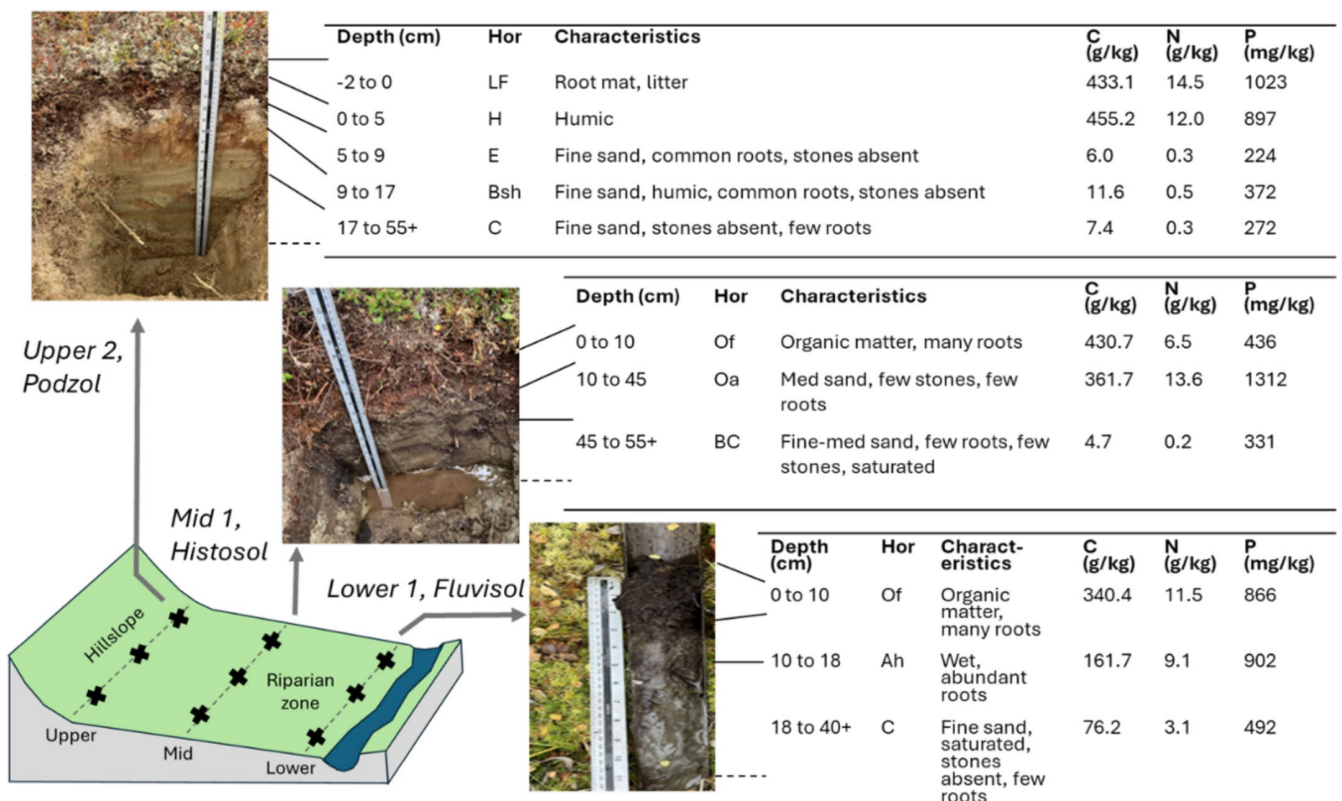


FIGURE 2 | A schematic of the sampling basis using lower (streamside), mid and upper landscape positions, showing representative soils and data from Cearrogeasjohka (Cea), photographs, and basic soil descriptions with total C, N, and P concentrations against depth. Soils in this example were classified as Podzol, Histosol, and Fluvisol (from upper to lower positions according to WRB major reference groups).



FIGURE 3 | Images of the landscapes of the four study locations (a) Cær, (b) Mar, (c) Ski, and (d) Dar.

HCl) and was found negligible (<0.5 mg/kg inorganic C). Total P was determined by a sodium hydroxide (NaOH) fusion method (Smith and Bain 1982) comprising ignition of 0.1 g samples with solid NaOH, titrating the melt to pH 7 with 20% sulfuric acid (H_2SO_4), and subsequent P analysis by inductively coupled plasma optical emission spectroscopy (ICP-OES; Agilent 7500ce instrument, Agilent Technologies, CA, USA). Oxalate extractable elements of P, Al and Fe (P_{ox} , Al_{ox} , Fe_{ox}) were determined by extraction of the soil with acid ammonium oxalate (Farmer et al. 1983) and analysis of the extract by ICP-OES. The P saturation index was calculated as the molar ratio $P_{\text{sat}} = [\text{P}_{\text{ox}}]/([\text{Al}_{\text{ox}}] + [\text{Fe}_{\text{ox}}])$. An internal reference soil included in triplicate achieved <5% relative standard deviation across triplicates in all analyses. Soil concentrations are reported based on dry matter (DM) basis (mg/kg or g/kg DM) following drying of a subsample at 105°C.

Water soluble nutrient forms were determined on 1 g (equivalent DM) air-dried, 2-mm sieved soil in 20 mL Milli-Q water, shaken by an orbital shaker at 200 r.p.m. for 16 h (20°C), centrifuged at 1500 g, and filtered <0.45 µm using GF/F filters into clean vials. Filtrates were analysed by automated colorimetry (Skalar San ++, the Netherlands) for nitrate-N ($\text{NO}_3\text{-N}$), ammonium-N ($\text{NH}_4\text{-N}$), total dissolved N (TDN), soluble reactive P (SRP; approximating to phosphate), total dissolved P (TDP), and DOC concentrations using an automated persulphate/UV digestion procedure. Colorimetric detection limits were 0.1, 0.01, and 0.001 mg/L for C, N, and P species, respectively. Dissolved organic nitrogen (DON) was calculated from the difference between TDN and the sum of dissolved inorganic N species ($\text{NO}_3\text{-N} + \text{NH}_4\text{-N}$) and molybdate unreactive P (approximating to dissolved organic phosphorus; DOP) was calculated as the difference between TDP and SRP. Soil pH was determined on fresh extracts at 1 g DM: 10 mL water ratios after 4 h of shaking. Absorbance of the soil water extracts was determined by UV-visible spectroscopy at 254 nm wavelength (Abs_{254} ; Spectra Max 190, Molecular Devices, CA, USA) using absorbance units (AU/cm), with specific UV absorbance determined as absorbance normalised to DOC concentration (hereby termed SUVA_{254} ; L/mg/m). Stoichiometric ratios of C:N:P in solid and aquatic phases were determined as molar ratios.

2.5 | Subsoil DOC Sorption Experiment

Experiments determined the sorption and filtration of topsoil DOC by subsoils in 2.5 cm diameter glass chromatography columns. A DOC solution of 57.2 mgC/L was water extracted (1 g DM:10 mL, filtered <0.7 µm) from topsoil organic horizons at Ski and compared to a 46.9 mgC/L characterised fulvic acid (FA) DOC standard solution (Filius et al. 2000).

Field-moist, sesquioxide-rich Bs horizon subsoil material from Tana subsoil (with Al_{ox} and Fe_{ox} concentrations of 1564 and 3145 mg/kg DM) was packed into two columns (A and B) to a depth of 2 cm (7.9 cm³) comprising 10.8 and 11.1 mg DM soil. After saturation with a 0.01 M NaCl priming solution (outflow end upwards) solutions were switched (determined as time zero) to the DOC extract and FA solution for columns A and B, respectively, at 0.1 mL/min. Sample fractions were collected

over 4 days, whereby 168 and 148 column pore volumes (PV) were the DOC sorption phase; then inflow was switched back to 0.01 M NaCl (desorption phase) up to a total of 239 and 210 PV. Column eluant fractions were analysed for Abs_{254} and concentrations of DOC, TDN, and TDP colorimetrically (Skalar San++). Full details are given in Supporting Methods of [Supporting Information](#).

2.6 | Data Analysis and Statistics

Basic exploration of relationships across all data was carried out using a standardised principal component analysis (PCA) based on a correlation matrix in Minitab (Minitab Inc. v17.1.0.0) and represented in a biplot. Statistical testing focussed on hypothesis testing of differences between soil horizons, sites, and within-site locations using a crossed design. Factor groups were (i) landscape position (pos; n=3) comprising lower (stream-side), mid, and upper positions and (ii) soil grouped horizons (hor; n=3) comprising organic topsoils (LF, H, and O horizons), topsoil, and near-surface mineral dominated layers (A and E horizons; hereby referred simply as mineral topsoil) and mineral subsoils (B and C horizons). Fixed effects testing (n=134 data rows) was carried out using an ANOVA general linear model in Minitab (v17.1.0.0) in the form Response variable=constant+hor+pos+site+hor*pos interactions (site*hor was not used in the model). All variables except pH were log₁₀ transformed. In total, we ran this test for 25 determinants, and thus we applied a Bonferroni correction for family-wise error to the significance level of 0.05. Statistical significance was 0.05/25=0.002 and was applied to ANOVA results and post hoc testing. Significance results (e.g., Table 3, Table S5) are presented as the ANOVA significance (in text and tables). Values passing the p<0.002 threshold are in bold in tables and noted as significant results text. Group differences were determined post-ANOVA using Tukey post hoc testing (99.8% confidence interval including the Bonferroni adjustment) and statistics are presented in Table S6, with plots of the confidence intervals around the mean in Figures S2–S4.

Soils were classified according to the World Reference Base (IUSS Working Group WRB 2022) based on field survey descriptions, images, and analytical data (pH and concentrations of C, Fe_{ox} , and Al_{ox}). Soils were grouped corresponding to the hydrology of soil types (HOST) classification (UK developed; Boorman et al. 1995) and their hydrological properties. This is latterly used to support the development of soil groups based on the prevalence of vertical and lateral soil water flowpaths. Soil stocks combined data from the overall horizon depth (or depth segments for multiple samples per horizon), stone-free bulk density values and total C, N, and P concentrations, then summed to a standardised 1 m depth (Tables S1–S4) based on site conditions indicating the lower horizon (e.g., B/C) extended to the 1 m depth, or for shallow soils a negligible contribution below the maximum sampled depth. Stone and rock contents were accounted for. Details are found in Supporting Methods of [Supporting Information](#). Differences in profile stocks between sites and positions were explored using ANOVA with Tukey post hoc testing at the p<0.05 significance level in Minitab.

TABLE 2 | Soil classifications using the World Reference Base for soils (WRB) classification (IUSS Working Group WRB 2022) with reference to field survey and analytical data (pH, organic carbon concentration, oxalate extractable Fe and Al). Dominant HOST (hydrology of soil types) soil water flow models are included with key at table base (models depicted Table S5).

Position	Classification criteria	Sites			
		Cær	Mar	Ski	Dar
Lower	WRB reference group	Fluvisol	Fluvisol	Fluvisol	Podzol
		Fluvisol	Fluvisol	Fluvisol	Fluvisol
		Fluvisol	Fluvisol	Fluvisol	Podzol
	Qualifiers	Gleyic, histic	Skeletal, gleyic	Eutric or dystric, skeletal	Skeletal, entic, albic
	Subqualifiers	Humic	Arenic, humic, folic	Siltic, clayic, arenic	Humic
	HOST models	G	E	E	E
Mid	WRB reference group	Histosol	nd	Podzol	Regosol
		Gleysol		Regosol	Podzol
		Gleysol		Regosol	Regosol
	Qualifiers	Eutric		Albic, skeletal, dystric	Leptic
Upper	WRB reference group	Siltric		Arenic, placic	
		J		A	H
		Podzol	Regosol	Podzol	Regosol
		Podzol	Regosol	Podzol	Regosol
		Podzol	Regosol	Arenosol	Regosol
	Qualifiers	Albic	Skeletal, eutric, brunic	Albic, dystric, brunic	Dystric, skeletal, brunic
	Subqualifiers		Arenic, folic, humic	Arenic, claric	Arenic, humic
	HOST models	A	H	A	H
Groundwater or aquifer					
Key to HOST models	Gleying or permeability	Groundwater normally > 2 m	Groundwater normally < 2 m	No significant groundwater	
	No slowly permeable, or gleyed layer < 1 m	Model A	Model E	Model H	
	No slowly permeable, or gleyed layer at 0.4–1 m	Minor presence		Not present	
	Gleyed layer < 0.4 m	Not present	Minor presence	Model J	
	Peaty topsoil	Minor presence	Model G	Not present	

3 | Results

3.1 | Soils in the Subarctic Riparian Plots

Figure 2 shows a representative soil plot and pit layout at the dwarf birch forest and mire site (Cær), with illustrative soil profiles showing a riparian transition from Fluvisols near-channel to Histosols (and some Gleysols) mid plot, and Podzols in the upper sites located at the base of the hillslope. Summary descriptions of soil profiles for Cær, Mar, Ski, and Dar are provided in Table 2 and full soil profile descriptions can be found in Tables S1–S4.

Fluvisols dominated the near-channel and depositional environment during spring melt-driven out-of-channel flood events at these small catchment scales. Fluvisols dominated the

near-channel positions at most sites indicative of depositional environments at times such as spring melt-driven out-of-channel flood events at these small catchment scales. The exception was Dar, where near-channel positions showed Podzols that indicated less channel influence on the surrounding land. The upper plot sampling positions were dominated by Podzols and either Regosols or Arenosols respectively, that is, soils with stronger (Podzols) and weaker development through processes such as weathering and vertical solute translocation. The mid-position sites had a variety of soils, with wetter Gleysols and Histosols at Cær and Podzols or Regosols at Ski and Dar.

Translation of soil profiles into the HOST classifications (Table S5, Table 2) shows soils of lower landscape positions were dominated by HOST class 7, with HOST 12 and 10 present

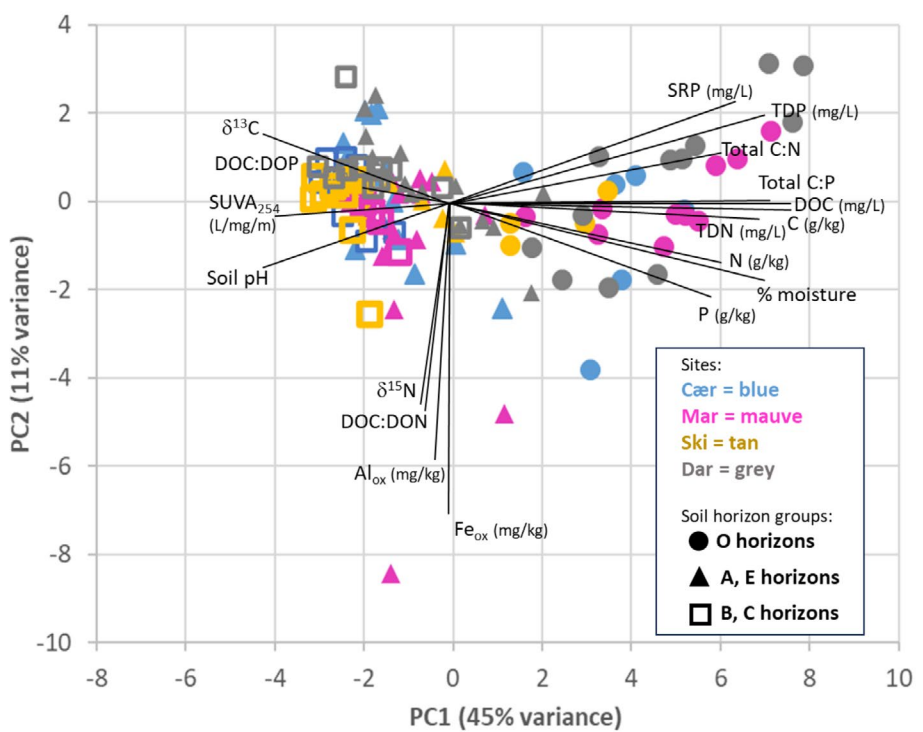


FIGURE 4 | Principal components biplot for all data separating out symbols for the three horizon groupings and colours for the four study locations of Cær, Mar, Ski, and Dar. The PC1 and PC2 refer to the first two principal components (with variance in brackets). Radial lines (length explaining weightning, direction explaining relative interaction with PC1 and PC2) use soil property naming as per Table 3.

in some lower transect points at Cær and Ski, respectively. Upper landscape positions showed consistent HOST class 5 at Cær and Ski, but class 17 at Mar and Dar. Mid positions were more variable: classes 15 and 24 at Cær, class 5 and 13 at Ski, class 17 at Dar (see Boorman et al. 1995 for class explanations). Explaining these classes using simplified HOST conceptual models shows that hillslope base soils at all sites showed no slowly permeable or gleyed layer within 1 m depth. At Cær and Ski, groundwater was expected normally > 2 m depth, leading to dominantly vertical unsaturated flow and some surface runoff (model A). Hillslope base soils of Mar and Dar had no significant groundwater (boulders at profile base), with vertical unsaturated and bypass flows in the profile and surface runoff likely (model H). The lower position soils were dominantly model E, having no slowly permeable or gleyed layer to 1 m, but groundwater present normally within 2 m, such that vertical flow occurrence and lateral flows to the stream change seasonally as to pathways deeper or shallower in the profile. Cær and Ski respectively showed peaty soil (model G) and gleyed mineral (model F) types also in the lower position, indicative of groundwater presence, seasonally saturated higher up the profile and vertical flow through topsoils to adjacent streams. Mid position soil translation showed more different water flow path groups. Mid positions at Dar (model H) and Ski (model A, one occurrence of model B showing seasonal saturated lateral flow) were the same as hillslope base positions. Mid positions at Cær (models D, J) showed gleyed mineral and peaty soils with prolonged seasonal saturated lateral flow. This conceptualisation is developed further in Section 4.4.

3.2 | Overview of Soil Properties and Relationships Amongst Variables

Full soil analytical data are given in Stutter et al. (2025). As well as the diversity of soils taxonomically, there was a considerable range in many of the analytical properties determined. The soils showed a range in stone-free dry bulk density of <0.1–1.9 g/cm³ across organic to mineral horizons, with soil moisture weight loss on drying 5%–91% of the field-moist soil. Soil pH ranged from 3.8 to 6.8. The ranges in total C, N, and P were 1–482 gC/kg, detection limit to 19 gN/kg, and 81–1312 mgP/kg, all expressed on a per dry matter basis. Very large ranges were found in oxalate extractable metals, notably Al_{ox} (178–21,885 mg/kg DM) and Fe_{ox} (52–17,459 mg/kg DM). Water extractable nutrients showed NO₃ concentrations consistently below detection limits (<0.02 mgN/L) but appreciable NH₄ (up to 2.5 mgN/L) and TDN (up to 13.5 mgN/L) suggesting high proportions of DON over inorganic N forms in many soils (mean sum inorganic N/TDN ratio of 0.11). Concentrations of SRP up to 14 mgP/L were greatest in organic topsoils and litter layers, with TDP up to 18 mgP/L and a smaller proportion of DOP (mean SRP/TDP ratios of 0.38). The range in water extracted DOC was <1–226 mgC/L and the mean and range in SUVA₂₅₄ of 3.3 (0.2–9.1) L/mg/m suggested an overall moderate to high aromatic character of DOC. There was no relationship between DOC concentration or SUVA₂₅₄ with Al_{ox} or Fe_{ox} (either individually or summed).

An initial PCA biplot (Figure 4) showed strong groupings by soil horizons and limited grouping for factors of site or

TABLE 3 | Testing for differences in soil characteristics from soil horizons (three groups), landscape positions (upper, mid, lower) and site effects (four subcatchments). Stated *p* values refer to ANOVA outputs, but bold font denotes results presented as significant following Bonferroni correction (see methods, cut-off *p* < 0.002). *F* values are given in full in Table S5.

Parameter group	Term	Horizon	Factor significance		
			Landscape position	Site	Hor × Pos
Macronutrient characterisation of soil solid phase	^{13}C	<0.001	<0.001	0.061	0.849
	^{15}N	0.053	0.307	0.131	0.150
	C g/kg	<0.001	0.001	<0.001	0.094
	N g/kg	<0.001	<0.001	<0.001	0.084
	P mg/kg	<0.001	0.008	<0.001	0.795
	Molar C:N	<0.001	0.045	<0.001	0.134
	Molar C:P	<0.001	0.368	0.049	0.861
Soil geochemical properties	Soil pH	<0.001	0.001	<0.001	0.229
	Al_{ox} (mg/kg)	0.551	0.286	<0.001	0.63
	Fe_{ox} (mg/kg)	0.523	0.001	<0.001	0.623
	Mn_{ox} (mg/kg)	0.003	<0.001	<0.001	0.359
	P_{ox} (mg/kg)	<0.001	0.338	<0.001	0.546
	Si_{ox} (mg/kg)	<0.001	0.070	0.019	0.010
	$\text{P}_{\text{ox}}/\text{Al}_{\text{ox}} + \text{Fe}_{\text{ox}}$ (molar)	<0.001	0.025	<0.001	0.358
Macronutrient characterisation of the water extractable phase	$\text{NO}_3\text{-N}$ (mg/L)	Model could not run (all values < D.L.)			
	SRP (mg/L)	<0.001	0.235	0.431	0.804
	$\text{NH}_4\text{-N}$ (mg/L)	<0.001	0.002	0.019	0.843
	DOC (mg/L)	<0.001	0.008	0.086	0.659
	TDN (mg/L)	<0.001	0.022	0.004	0.079
	TDP (mg/L)	<0.001	0.042	0.062	0.573
	DON (mg/L)	<0.001	0.037	0.002	0.051
	DOP (mg/L)	<0.001	0.102	0.002	0.156
	Molar DOC:DON	<0.001	0.138	0.016	0.042
	Molar DOC:DOP	<0.001	<0.001	0.057	0.194
	SUVA@254 (L/mg/m)	<0.001	0.099	0.002	0.020

landscape position. The first axis explained 45% of the variance and clearly separated out organic topsoil (O, H and LF) horizons from subsoil (B, C), with mineral near-surface and topsoils intermediate (A, E horizons). Main negative loadings on the first axis, with leverage on the positioning of mineral soils, were $\delta^{13}\text{C}$, SUVA₂₅₄, and soil pH. Positive loadings, related to C, N, P concentration metrics in total and dissolved forms, were linked to the separation of organic topsoils. The second axis explained only 11% of the variance and differentiated mineral topsoils specific to site Mar associated with their concentrations of Fe_{ox} and Al_{ox} .

3.3 | Concentration Changes in Soil Total C, N, and P and Geochemical Properties Between Horizons, Landscape Positions, and Sites

Total C, N, P concentrations in the soils were generally dependent on soil horizons, landscape position, and sites, with non-significant interaction effects (Table 3). Soil geochemical properties were mostly differentiated by sites, while macronutrient characterisation of the water-extractable phase was mostly dependent on soil horizons (Table 3, Table S6). Group mean values and post-ANOVA Tukey comparisons within the factors

are given in Table S7. Results are presented as significant only if passing the Bonferroni-corrected threshold of $p < 0.002$.

Total concentrations of C, N, and P showed a significant influence of horizon and site (all $p < 0.001$). For C and N concentrations, landscape position was a significant control. Total C and N concentrations declined through the soil profile with organic topsoil > mineral topsoil > subsoil (group means of 342, 22, 6gC/kg and 11.7, 1.1, 0.3gN/kg, respectively). For P, declines with depth in mineral soils were not pronounced and followed the order: organic topsoil (759mgP/kg) > mineral topsoil (331mgP/kg) = subsoil (339mgP/kg). Macronutrient ratios varied significantly by horizon ($p < 0.001$), with molar C:N greater only in the organic topsoil than in other horizons, whereas C:P declined with depth. In terms of landscape position, total C and N concentrations showed consistent differences: lower (streamside) position > mid, but upper was not distinct from other positions. Landscape position was not a significant control on total P concentrations, molar C:N, or C:P. The stable isotope ratio $\delta^{13}\text{C}$ values showed a significant difference ($p < 0.001$) between soil horizon groups, being less negative in deeper mineral horizons and a significant difference between landscape positions ($p = 0.001$), being more negative in lower positions than in mid and upper. Delta ^{15}N showed no significant horizon or position differences.

Soil pH showed a significant difference only in the organic horizons ($p < 0.001$), with organic topsoil (group mean 4.42) < mineral topsoil (5.24) = subsoil (5.50). Landscape position was a significant control ($p < 0.001$) on soil pH: lower (5.29) > upper (4.95), but mid (4.93) not different to other positions. Oxalate extractable elements (denoted X_{ox} ; Table 3 and Tables S6 and S7) were associated with amorphous (non-crystalline) precipitates (e.g., goethite, ferrihydrite) on soil surfaces that control anionic sorption (e.g., PO_4^{3-} and charged DOC). Horizon was a significant control ($p < 0.001$) on P_{ox} , Si_{ox} , and the P saturation of anion exchange sites ($P_{\text{sat}} = (\text{P}_{\text{ox}}/\text{Al}_{\text{ox}} + \text{Fe}_{\text{ox}})$), but was not significant for Fe_{ox} , Mn_{ox} and Al_{ox} . Tukey post-ANOVA testing showed three patterns of depth control: (i) decreasing values organic > mineral topsoils = subsoils for P_{sat} , (ii) for P_{ox} and Mn_{ox} organic > subsoil, but mineral topsoil was not distinct, and (iii) increases organic < mineral topsoil < subsoil for Si_{ox} . Landscape position was a significant control ($p < 0.001$) on Fe_{ox} , Mn_{ox} (with lower > upper, but mid not different to other positions), and was not significant for Al_{ox} , P_{ox} , Si_{ox} , or P_{sat} .

Interpretation of the effects of site location is complicated by the ability to sample to varying depths and is not considered in detail here (but are discussed in terms of stocks to a fixed soil depth; Section 3.5). For example, Dar showed equal greatest total C and N concentration (with Cær), but the bouldery subsoils meant that sampling was limited to topsoils and not lesser C and N concentration subsoils.

3.4 | Concentration Changes in Water Soluble DOC and Dissolved N and P Forms Between Horizons, Landscape Positions and Sites

Soil horizon was a significant control ($p < 0.001$) on soil water extraction concentrations of C, N, and P forms, macronutrient

molar ratios, and SUVA₂₅₄ (Table 3 and Tables S6 and S7). The exception was NO₃ concentrations (consistently below detection limit; 0.1mgN/L). Four patterns of depth effect were evident from Tukey testing: (i) a steep concentration decline with depth: organic > mineral topsoil > subsoil for NH₄, DOC, TDP, and DOP, (ii) a moderate decline from organic topsoils into mineral soils: organic > mineral topsoil = subsoil for SRP, TDN, and DON, (iii) a decline from organic topsoils to subsoil for molar DOC:DON, and (iv) a depth increase: organic < mineral topsoil = subsoil for molar DOC:DOP and SUVA₂₅₄. The SUVA index showed increasing aromaticity of DOM from 1.7, 3.2, and 3.5L/mg/m in organic, mineral topsoils, and subsoil, respectively. Examples of variables fitting pattern (i) were DOC (60, 12, 4mgC/L, for organic, mineral topsoils and subsoil, respectively) and TDP (1.62, 0.14, 0.05mgP/L). Examples of variables fitting pattern (ii) were SRP (0.048, 0.024, 0.020mgP/L) and TDN (3.8, 1.1, 0.7mgN/L). The greater organic topsoil values of water-extractable DOC:DON approximated the depth pattern of total soil C:N ratios, although at a slightly greater ratio for the solutes. Conversely, solute DOC:DOP ratios that were smaller in organic topsoils (182) than mineral topsoil and subsoil (339–490) opposed the larger total soil C:P ratios in the organic topsoil (1175) compared to mineral topsoil and subsoil (331–339). This suggested that the apparent total ecosystem resources of C relative to P did not translate to such a large excess of bioavailable (soluble) C relative to P.

Landscape position showed no significant control on any water-extractable nutrient concentrations. Only the DOC:DOP ratio showed landscape position as a significant control ($p < 0.001$).

3.5 | Soil C, N, and P Soil Stocks

Stocks calculated to 1 m soil depth (or lowest depth of soil onto boulders) showed a range in C of 2.28 (Ski, mid) to 28.09 (Cær, lower) kgC/m², a range for N of 0.11 (Ski, upper) to 1.19 (Cær, lower) kgN/m² and for P a range of 0.04 (Dar, mid) to 0.88 (Cær, mid) kgP/m² (Table 4). Significance of site and landscape position was explored using a two-way ANOVA (overall model adjusted R^2 of 38%, 52%, and 46% for C, N, and P stocks, respectively). Site was not a significant control on C ($p = 0.04$) and N ($p = 0.006$) stocks, considering our more stringent application of the Bonferroni corrected significance threshold of $p < 0.002$. However, for P stocks ($p < 0.001$) site differed: Dar < Cær = Mar = Ski. Landscape position was a significant control on C and N stocks, but was not significant for P stocks. Soil C and N stocks ($p = 0.002$ and < 0.001 , respectively) showed consistent patterns with position: lower > mid = upper. For C stocks, group means for landscape positions were 14.1, 7.2, and 6.8 kgC/m² and for N were 0.66, 0.33, and 0.32 kgN/m², for lower, mid, and upper, respectively.

3.6 | Subsoil DOC Interactions

Two column experiments were carried out to determine the DOC interaction potential with subsoil. The column A experiment exposed native River Tana watershed soil DOC (topsoil water extract; 57.2mgC/L) to Tana Bs subsoil material over 128 column pore volumes (PV) and 74h. The column B experiment exposed

TABLE 4 | Stocks of macronutrients in the River Tana watershed determined for soil profile locations and sample numbers (in italics) for chemical and bulk density (BD) samples, respectively (where discrepancies indicate missing BD determined from a model relationship between SOC and measured BD).

Site	Cær		Mar		Ski		Dar	
	Cærrogæs Johka		Mareveadji		Skierrejohka		Darjohka	
	kg/m ²	n						
C	L1	28.09	3, 3	8.61	5, 5	10.93	2, 2	14.05
	L2	18.95	3, 3	7.35	4, 3	20.44	2, 2	11.53
	L3	13.25	5, 5	14.88	4, 3	21.57	2, 1	13.69
	M1	26.12	3, 2	nd		2.28	4, 3	8.22
	M2	6.40	3, 3	nd		3.41	3, 2	7.42
	M3	9.52	4, 3	nd		10.61	4, 4	7.16
	U1	10.23	4, 4	8.12	3, 2	2.29	4, 3	3.87
	U2	13.62	4, 4	7.08	2, 2	7.94	3, 3	7.80
	U3	7.47	4, 4	12.89	4, 3	2.60	3, 3	9.29
N	L1	1.19		0.44		0.52		0.66
	L2	0.90		0.54		0.86		0.52
	L3	0.82		0.63		0.78		0.47
	M1	0.83		nd		0.12		0.37
	M2	0.26		nd		0.17		0.46
	M3	0.47		nd		0.40		0.35
	U1	0.53		0.36		0.11		0.20
	U2	0.55		0.33		0.36		0.39
	U3	0.43		0.40		0.12		0.43
P	L1	0.71		0.27		0.07		0.13
	L2	0.22		0.32		0.07		0.09
	L3	0.20		0.33		0.08		0.12
	M1	0.16		nd		0.28		0.05
	M2	0.88		nd		0.23		0.06
	M3	0.78		nd		0.35		0.04
	U1	0.36		0.19		0.45		0.13
	U2	0.39		0.13		0.40		0.05
	U3	0.48		0.23		0.37		0.16

a redissolved FA standard (46.9 mgC/L) to the same Bs horizon material over 113 PV. The Tana topsoil DOC had a SUVA₂₅₄ of 2.9 L/mg/m and the fulvic standard 2.6 L/mg/m. The sorption phase led to 30% overall retention of the Tana topsoil DOC mass and 48% of the fulvic standard DOC mass in the subsoil column (maximum sorption 0.47 and 0.88 mgC/g soil DM, respectively). A subsequent desorption phase (DOC feed solution replaced with 0.01 M sodium chloride (NaCl) over ~100 PV) led to 7% and 2% of the retained C mass being desorbed from column A and B, respectively.

The outflow concentration (for a given time, relative to inflow; C/C_0) for DOC showed a log function with a fast initial rise, then a slowing rate to a maximum of ~0.9 and ~0.5 for the Tana topsoil and FA standard DOC, respectively (Figure 5a). Hence, the Tana topsoil DOC remained more mobile in the sesquioxide-rich Bs subsoil matrix than the FA standard DOC. Consequently, total C mass sorbed at the maximum PV according to the fitted regression model in Figure 5b was greater (6 mg) for the FA standard than the Tana topsoil (4.5 mg). Despite a higher value of Abs₂₅₄ for the Tana topsoil DOC inflow solution than the FA standard (1.7 and

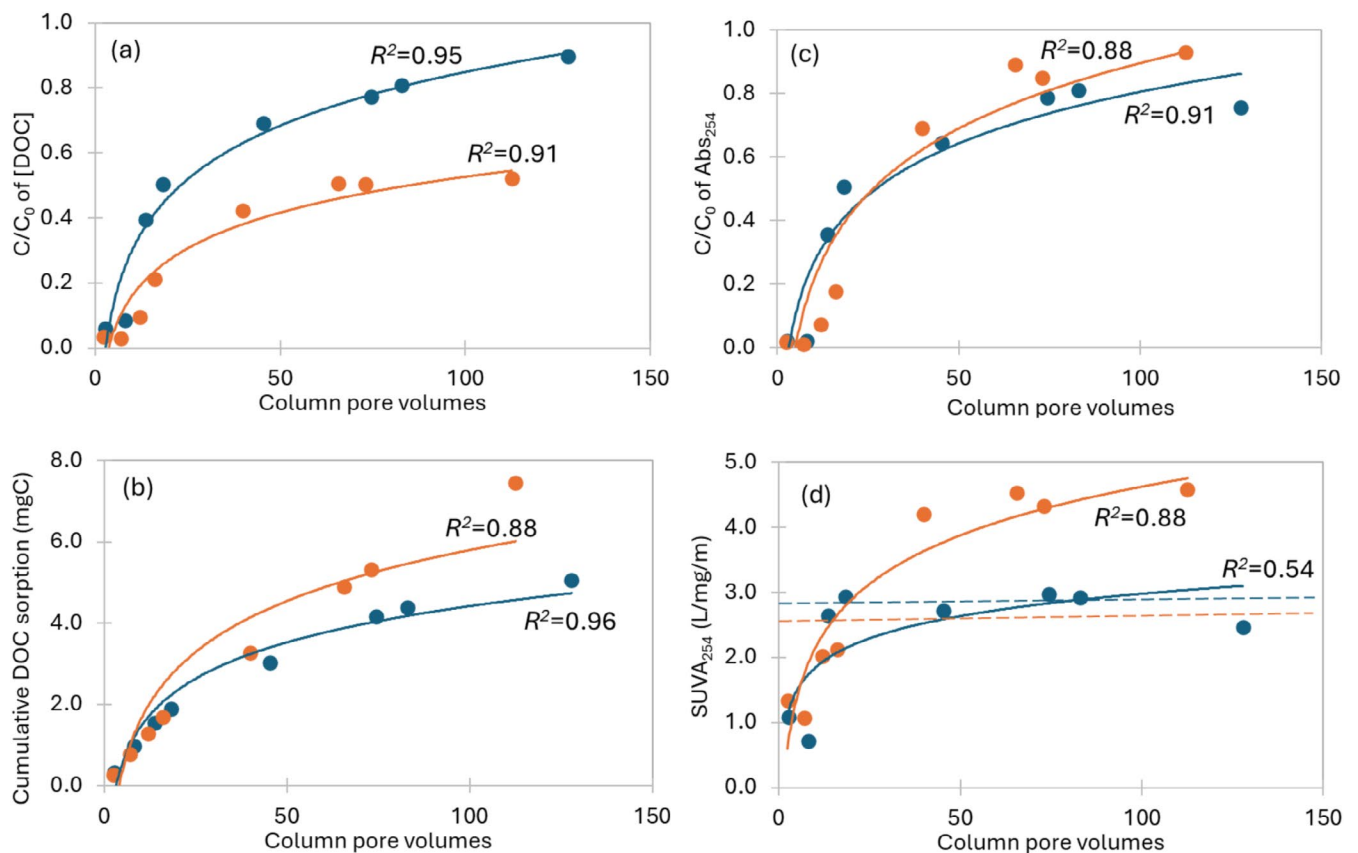


FIGURE 5 | Change in column eluant properties during the sorption phase for exposure of River Tana topsoil DOC (blue lines) and fulvic acid standard DOC (orange lines) to Tana Bs subsoil. (a) C/C_0 concentrations of DOC, (b) time course of C mass sorbed, (c) C/C_0 of absorbance at 254 nm (Abs₂₅₄) and (d) Specific UV Absorbance (SUVA₂₅₄) where the reference (dashed, horizontal) lines equal the inflow SUVA₂₅₄ value. Where C/C_0 is the column outflow concentration at a given pore volume normalised to the concentration of the inflow solution.

1.2 AU cm⁻¹), over time, the column eluant UV absorbance was similar (Figure 5c). However, the eluant showed lower SUVA₂₅₄ values for the Tana topsoil DOC over time, which then stabilised to the inflow SUVA₂₅₄ after 120 PV. Conversely, the column eluant SUVA₂₅₄ of the FA standard treated column exceeded the SUVA₂₅₄ of the column inflow after only 20 PV (Figure 5d).

4 | Discussion

4.1 | Controls of Site, Landscape Position, and Horizons on Soil Properties

Riparian and hillslope base soils differed at many sites. Soil WRB classifications (Table 2), informed by field and laboratory data, showed Fluvisols exclusively at near channel positions of sites Cær, Mar, and Ski, demonstrating current fluvial processes have an influence on soil formation at 34–68 km² river scales. The mid landscape position varied in soil types between sites. At Cær, restricted soil vertical drainage associated with fine texture, high density subsoil led to mid position development of Histosols and Gleysols. A narrow riparian zone at Mar related to valley configuration. The mid plot positions of Ski and Dar had Podzols and Regosols like the hillslope base. The transition differed at the upland Dar site (smallest catchment), where immature soils were present with less horizon development (Regosols and weakly developed Podzols).

Spatial differences were observed in chemical soil properties across the groups of soil total and water-soluble nutrients, and surface sorption characteristics (Table 3 and Tables S5 and S6). Compared to other transect positions, near channel soils had greater pH (more alkaline), larger concentrations of C, N, amorphous Fe (Fe_{ox}) and water-soluble NH_4^+ and DOC than soils at upper landscape positions. Overall, soils at mid landscape positions showed more similarity to upper positions, often significantly different in properties from streamside lower positions. Quantification of total and labile forms of soil macronutrients is important in understanding catchment source areas and their vulnerability to change, hydrologic connectivity, and influence on river processes. Knowledge of solid and solution phase organic matter protection with soil mineral surfaces such as calcium bound forms and Fe and Al oxides/oxyhydroxides (Wieder et al. 2019) is important to reduce uncertainty in SOM decomposition.

Broll et al. (2007) studied a headwater catchment in Fennoscandia (Tenojoki, River Tana; 69°50', 300–420 m altitude) with a soil mosaic of Podzols and hydromorphic soils, noted to respectively correspond to a gradient from lichen to dwarf shrub to grass bog vegetation. Our site descriptions aligned that site to Dar in the present study. Only the topsoil (O and A horizons) was investigated but soil organic carbon (SOC) ranged from 30% to 45% and ~5% in O and A horizons, respectively, on the valley floor, whilst on the slopes 15%–40% and 5%–10% in O and A horizons. The

C:N values ranged from 20 to 50 and ~15 in O and A horizons, respectively, on the valley floor, whilst on the slopes 20–35 and 18–25 in O and A horizons. In the present study landscape position strongly influenced SOC concentrations, but not C:N ratios.

Broll et al. (2007)'s conceptualisation of the hillslope transition comprised: (i) freely drained Podzols on hilltops, and on convex slopes with dwarf shrub and mountain birch, (ii) Podzols on the slope-foot zone with moderately well-drained hummocks (cryoturbated) and poorer drainage in troughs, supporting dwarf birch (*Betula nana*), willow shrub (*Salix glauca*, *Salix lapponum*) and mosses, then (iii) a valley floor (our 'riparian zone') comprising poorly drained hummocky organic soils, to (iv) narrow stream-side floodplains of poorly to very poorly drained humus-skeletal soils with sedges and willow shrub, with occasional patches of bog peat soils (sedges, cotton grass, mosses). A sharp gradient of soil moisture from low on tops and hillslopes to high on the footslope-valley floor, demarcated two ecotones, accompanied also by more consistent temperate regime in the lower zone and base cation saturation (from seepage from hillslopes). These factors support the inference of an enriched bioactive zone in the valley bottom with conditions more conducive to higher biogeochemical process rates. The present study supports that forest and dwarf forest/tundra sites have active riparian zones enriched in nutrients, but not the case for the mountain sites (Dar).

Data on N, and especially P, is less commonly reported than for SOC. Uhlig et al. (2004) examined Podzols under lichen heath and dwarf birch communities in the Tana catchment (69°, 13–22' N) seeking to contrast controls against sites overgrazed by reindeer, including soil pit description to 80 cm depth (aligned with sites Cær and Ski in our study). Data from Uhlig et al. (2004) show plant available N (Kjeldahl-N) ranged from 0.9% to 1.5% in the O horizons, 10-fold less in E horizons and <0.05% in B horizons. These authors' approximate means for total P (method unstated; data from graphs) for control sites were 850, 30, and 360 mgP/kg (DM) for O, E and B horizons and plant available P approximated 160, 5 and 10 mgP/kg (DM). In comparison, our study found similar total P of 760 and 339 mgP/kg for organic topsoil and subsoil (combined B and C horizons), respectively (Table S6), but greater concentrations of 331 mgP/kg for combined A and E horizons.

4.2 | Comparisons of Soil C, N, and P Stocks to Other Arctic and Temperate Systems and Role in Overall Ecosystem Nutrient Balances

We evaluated the C, N, and P stocks of the soils in the River Tana against other literature derived stocks for high latitude systems (Table 5). Batjes (2002) gives general context to these values with an inventory of mean European soil C and N stocks, where Podzols, Regosols, and Fluvisols were 29.6, 10.4, and 21.9 kgC/m², respectively, and 2.0, 1.1, and 3.5 kgN/m², respectively, to 1 m depth. Our data show mean values of 11 kgC/m², similar to European average Regosols (often in headwater landscapes) and lower N stocks at 0.5 kgN/m². The mean and range of C for our sites combined were lower than many other studies in arctic regions and less than studies by Kjellman et al. (2018) and Kjær et al. (2024) in the Tana catchment which targeted peat

TABLE 5 | Comparison of data on soil C, N and P storage in soils [mean (range)] from the River Tana watershed with data reported from published literature for subarctic to arctic regions.

Source	C stocks (kg/m ²)	N stocks (kg/m ²)	P stocks (kg/m ²)	Investigated site and soils
This study (0–100cm)	Mean 10.84 (2.28–28.09)	Mean 0.48 (0.11–1.19)	Mean 0.27 (0.04–0.88)	Riparian-hillslope transition soils, Tana catchment, Finmark, Norway (69°N)
Kjellman et al. (2018)	56–156	4.6, derived from pooled sites mean data		Tana catchment, Finmark, Norway (69°–70°N). Four permafrost peat soils (84–229 cm depths)
Kjær et al. (2024)	Mean 96 (62–143), derived from reported data	Mean 3.6 (2.4–4.4), derived from reported data	Mean 0.11 derived from reported data	Tana catchment, Finmark, Norway (69°–70°N). Three permafrost-thermokarst peat soils (85–150 cm depths)
Mueller et al. (2015)	Mean 46 (37–57)	Mean 2.6 (1.9–3.1)		Alaksa (71°N), historic large, drained lake basins, <i>Aquorthels</i> , <i>Aquiturbels</i> , <i>Historthels</i>
Alekseev and Abakumov (2022)	Mean 24.0 (16.3–34.0)			Western Siberia (66°–68°N), Cryosols
Obu et al. (2017)	Mean 38.7 (5.5–91.0)		Mean 0.8 (0.2–1.5)	Herschel Island, West Canada (70°N), Cryosols
Ping et al. (2008)	Mean 11.0 (0.3–19.8)			Alaska and Canada, (67°–70°N)
Ola et al. (2022)	15.7–82.0		1.0–4.0	Bylot Island, Greenland (73°N), Cryosols

Note: Soil classifications given relate to those in the cited studies and use differing systems. Classifications using WRB (common to general usage in this study) are in plain font and those in italics use USDA soil taxonomic classification (Soil Survey Staff 1999).

soils subject to permafrost thaw. Devos et al. (2022) studied soil C stocks in surface soils (O and A horizons only) across Norway (10 out of 14 sites above 67°N latitude) comparing mountain birch forest and tundra across the treeline. These authors found forest had greater C stocks than tundra (respective medians of 2.02 and 1.33 kgC/m²) but when considering amongst-site variation they concluded vegetation was a minor factor explaining differences in soil C and elevation, slope and temperature were of greater importance.

Soil C stocks from our sites were similar to Siberian Cryosols (similar latitude) studied by Alekseev and Abakumov (2022) and to Alaskan and Canadian soils studied by Ping et al. (2008). Soil N stocks from our study were similar to those of Cryosols in Canada (70°N) studied by Obu et al. (2017), but less than other reported arctic soils, including the peats in the Tana region. Total P stocks were seldom reported in other studies, but the mean 0.3 kgP/m² from our River Tana sites was more than double the value reported by Kjaer et al. (2024).

A report on C storage in Norwegian ecosystems (Bartlett et al. 2020) does not separate (nor mention) riparian ecosystems. In general, high latitude European soils are poorly represented in soil databases or mapped at a coarse scale since resources focus on productive soils. Hence, data on properties such as soil nutrient stocks contribute to sparse knowledge and collectively can inform modelling.

4.3 | Surface and Subsoil Interactions Governing Landscape Nutrient Transfers

Generally, macronutrient concentrations declined with depth in soil profiles for total C and N, with larger total P concentrations in organic surface than underlying mineral soils, supporting that organic matter enriched surface layers are dominant sources of nutrients. Furthermore, mean data for DOC, TDN, and TDP all show similar declining concentrations as a function of depth. This conforms to the dominant source layer concepts developed for boreal forest soils (Lidman et al. 2017) in which lateral transport of DOM towards the stream is maximised when water tables reach near-surface horizons containing large DOM concentrations. As an example, Lower 1 soil at Cær (histic, gleyic Fluvisol) yielded 79 mgC/L water extractable DOC in the Of horizon at 0–10 cm depth, with common saturated conditions leading to lateral near-surface flows (Host model D; Table 2). The soil HOST translation suggests diverse flow conditions influencing solute delivery from surface sources towards the drainage network, laterally (dependant on water table seasonality) or to deeper pathways encountering mineral surfaces where sorption can slow and filter charged anionic forms of DOM and phosphate. Subsoil interactions depend on the flow routing (Section 3.1, developed further in Section 4.4), and sorption chemistry of surfaces. Oxide forms of Al and Fe are known to control sorption, especially under conditions of low in situ organic matter production (Kawahigashi et al. 2006). Although sorption complexes (measured as Al_{ox}, Fe_{ox}; Table 3 and Table S6) did not vary significantly with soil layers, the large concentrations in Podzol mineral horizons (up to 3 g/kg) suggest anion retention. Significantly larger mean concentrations in the lower transect position sites (Table 3) may be related to

barriers in downward percolation of waters carrying Fe²⁺ under saturated melt conditions on floodplains then subsequent oxidation during low rainfall summers (as seen in permafrost regions; Alekseev et al. 2003).

Our column experiments showed that 30% of the surface soil water-extracted DOC was sorbed onto a podzolic subsoil and that, under the physico-chemical conditions of the column experiments, this was not readily reversible (7% of C mass sorbed became desorbed; Figure 5). The maximum sorption of Tana topsoil DOM of 0.47 mgC/g soil DM in the present study was at the upper range (0.15–0.63 mgC/g soil DM) found by Lim et al. (2022). These authors passed topsoil DOM (at near identical concentration to our experiment) through E and B horizon subsoils from Siberian discontinuous permafrost peatlands (forest-bog biome) and found maximum adsorption for sandy texture Al-Fe-rich Bs horizons. Similar to the present study, these authors found increasing SUVA₂₅₄ as sorption increased, indicating initial retention/retarded transport of more aromatic, potentially larger molecules, with diminishing effect over time (SUVA between 2 and 5 L/mg/m for the Bs horizon in Lim et al. (2022) and 1–3 L/mg/m in the present study; Figure 5d).

Free-draining soils (hillslope base Podzols, Regosols, Arenosols) with percolation of surface-derived DOM downwards to mineral horizons were indicated as prevalent at Cær and Ski (upper position HOST model A) and possible at Mar and Dar (HOST H). These, and lower landscape positions with seasonal periods of surface to subsoil connectivity (HOST E) have subsoil potential to retain DOM and alter amounts, and selectively forms of DOM transported to streams. Qualitative changes in DOM quality, that is, its composition characteristics, were indicated with increasing Abs₂₅₄ and SUVA₂₅₄ values over time (column effluent compared to influent), and their values stabilising to the reference FA at the end of the experiment. This indicated initial retention of aromatic DOM composition (and potentially larger molecular weights) that took longer to pass through the column (i.e., preferentially retained on the subsoil). Kawahigashi et al. (2006) proposed the concept that DOM sorption and filtration were maximised in Inceptisols (equivalent to WRB-defined Regosols in the present study) in permafrost regions of Siberia (65°N), where hydrophobic (H_{phob}) DOM sourced in organic surface horizons is enhanced by hydrophilic (H_{phil}) DOM from mineral topsoils, then, following infiltration into deeper active layers, has selective removal of H_{phil} DOM in subsoils.

Questions remain to translate the column simulation data to landscape scale DOM delivery processes, namely: what are landscape path lengths for subsoil transport from DOM sources to watercourses; what are timescales for source mass loads that approach saturation of subsoil sorption; what biogeochemical interactions in situ influence sorption reversibility? Catchment DOM modelling should incorporate best soil chemistry and transport process knowledge. The combination of reactive subsoils with respect to DOM sorption, coupled with soil morphology and flow conceptualisation, suggests large potential for interruption and alteration of DOM transport from catchment uplands. In such subarctic landscapes, this may infer a heightened importance of near-stream areas of continuous or seasonally elevated water tables as sources of larger DOM loads, or

DOM forms with specific roles in aquatic ecosystems and the land-water-air-ocean continuum.

4.4 | Informing a Conceptual Understanding of Interactions Between Soils and Runoff Relating to Subarctic Catchment C, N, P Sources

As we continue to make biogeochemical connections between terrestrial and aquatic watershed components, an overarching question is: how can soil data improve catchment biogeochemical modelling of DOM source and fate in subarctic systems? Berggren et al. (2022) argue that aquatic DOM turnover rates are governed by interacting intrinsic (inherent molecular properties) and extrinsic factors. The latter include temperature, climate, light, supply of other nutrients, and biological community present. They act in conjunction on major biogeochemical aspects such as bioreactivity, flocculation, and photo-processing in freshwaters. Within such a framework, they suggest (i) that catchment dynamics of water residence time and hydrological connectivity integrate many intrinsic and extrinsic factors, whilst (ii) intrinsic factors dominate DOM turnover in small headwaters and progressively extrinsic factors dominate at increasing river sizes (greater in-river processing).

Our data cover ecosystem zones of tundra, forest, and mountain; covering scales where high connectivity of streams to land was found (Table 1) and supporting other project activities using long-term sensor deployment in streams. Deep peat mire soils were not sampled directly in our study, although present in some of our subcatchments (13% in Mar and Ski, 5% in Cær). To include them in our conceptual understanding, we used data from the literature (Table 5).

River reaches adjacent to sampled soils were surveyed for lateral inflows by in-stream tracer studies (Table 1), but we lack consistent direct data in this study on the in situ transport regime of the studied soil types. Our results showed heterogeneity between stream segments adjacent to the soil sample locations that were gaining and losing flow within close distances, suggesting discrete lateral inflows from riparian soils, two-way exchanges and lateral or vertical exchanges (Gomez-Velez et al. 2015). Such processes likely increase DOM source-stream connections, contributions and water residence times for DOM processing (Ryan et al. 2024; Liu et al. 2022). Our stream hydrochemical data for comparison with soil data is limited. Arctic systems exacerbate such study difficulties and reinforce the need for modelling approaches to advance research of catchment-scale DOM dynamics. Such models will need to parametrise runoff generation, hydrological response units intersecting source units of varying C, N, and P stocks, water travel times and seasonality, and measurements of DOM molecular composition by advanced analytical chemistry molecular-level techniques such as high-resolution mass spectrometry.

Figure 6 conceptualises major soils of the River Tana (both directly sampled and inferred for mires) combining knowledge on soil classifications, flowpaths, and compositions. Towards supporting semi-distributed subarctic catchment DOM models, we propose four major headwater hillslope-riparian units (left to right; Figure 6): Groups (1) the afforested, floodplain soils (Fluvisols) and (3) mountain soils share characteristics of flow contributions through topsoils, moderate influence of subsoils on DOM, and diffuse DOM inputs by groundwaters (with moderate subsoil DOM filtering; Figure 5). The difference between (1) and (3) is the greater C source (related to stock and C-density data) in the lowland floodplain forest than upland mountain

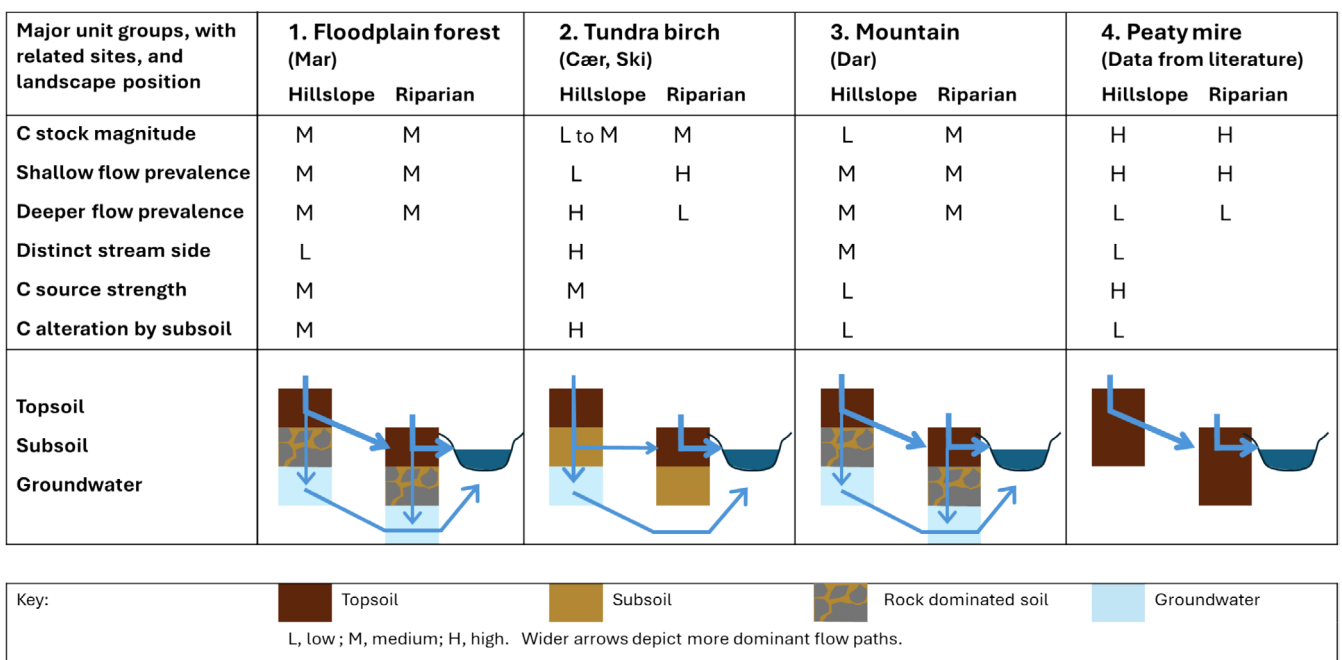


FIGURE 6 | Conceptual illustration of hillslope base to stream side riparian transitions representative of subarctic European catchments combining data from the River Tana watershed and literature (peat dominated areas) to understand spatial units of source-transport of dissolved organic matter to rivers.

zone. Group (2) the tundra birch upland zone (combining data from Cær and Ski) differed from the forested alluvial soils in two important ways (i) that riparian and streamside soils were variably with often saturated lateral flow through surface horizons indicated as large potential DOM sources, and (ii) that dominantly vertical transport on the hillslopes brought any DOM enriched waters in contact with subsoils with high potential for DOM sorption and fractionation. Group (4) mire soils, not studied in the current study, were inferred from literature data (Table 5) and knowledge of peats elsewhere (Boorman et al. 1995) as the highest C stocks, but with only active transport and flushing in surface layers. Although C stocks are large in the riparian peat soils when compared to organo-mineral soils, these are often disconnected from transport by the low hydraulic conductivity of the peat matrix below the immediate surface.

The extrinsic factors in DOM cycling noted by Berggren et al. (2022) are changing in arctic systems. Our data inform such frameworks for DOM cycling in large arctic riverscapes in several ways: (i) by examining DOM sources in near channel soils highly connected to headwaters (lower order channels), (ii) understanding amounts and bulk quality (e.g., Abs₂₅₄, SUVA₂₅₄, and stoichiometry) of potentially transported DOM, and (iii) relating soil properties to interactions such as potential DOM mobility, sorption, and alteration of DOM form. There is clear role for combining soil biogeochemistry and hydrology to look inside the catchment ‘box’ to better understand DOM cycling in changing ecosystems. A key stage will be to make clear links between DOM quantity, quality between soils and surface waters and timing of delivery. This could usefully include molecular compositions of riparian soil and waters from headwaters to longer river transects.

5 | Conclusions

Our study informs catchment DOM processes from soils to waters in the latitudinal band of subarctic ecosystems. The underlying premise was that riparian soils exert a disproportionate influence on river exports of DOM due to their hydrological connectivity to channels, distinct source areas, and as reactive interfaces to upslope contributions. In characterising hillslope-to-riparian transitional soils in the subarctic River Tana catchment, we found considerable variability amongst sampled headwaters (3rd order streams; 31–64 km² catchments). Strong horizon-based differences in total C, N, P concentrations and soluble macronutrients were shown by the dominantly organo-mineral variants of Fluvisols, Gleysols, Podzols, and Regosols, alongside differences between sites. Wetter riparian and streamside positions had enhanced C, N, and DOC concentrations. Stocks of C, N, and P were highly variable, greatest in riparian positions in the plateau tundra sites. Such soils are rarely described in terms of combining C, N, and P data together. Data show that often P stocks were equal to that of N, suggesting moderate P and low N supply to ecosystems. Unlike peat soils that have potentially larger C stocks, these organo-mineral soil transitions show important interactions between surface and subsoil pathways capable of altering DOM.

To support semi-distributed modelling of DOM cycling in subarctic ecosystems, we attempted to contrast simplified soil differences across the dominant ecosystems of mountain,

plateau dwarf forest tundra, and floodplain birch forest using our data, supplemented by literature data on mire soils in the area. Differences in flowpaths and interactions with varying horizon C, N, and P concentrations were conceptualised by soil type zones that can inform source-transport and hydrological response unit structures in catchment models.

We conclude from the differences observed that data and knowledge on near-channel soil processes will help connect river biogeochemical study of DOM origins and fate across scales in large subarctic (and perhaps arctic) rivers. The challenge is to simplify landscape soil complexity using frameworks like hillslope–riparian units that provide close linkages to processes needing to be incorporated into dynamic DOM process models to understand responses of arctic ecosystems to change.

Author Contributions

Marc Stutter: conceptualization, investigation, project administration, writing – review and editing, writing – original draft, funding acquisition, formal analysis, methodology, data curation. **Leah Jackson-Blake:** conceptualization, investigation, writing – review and editing, project administration. **Maeve McGovern:** conceptualization, writing – review and editing, investigation, project administration. **Juliana D'Andrilli:** conceptualization, investigation, writing – review and editing, project administration, funding acquisition. **James R. Junker:** conceptualization, investigation, project administration, writing – review and editing. **Peter Dörsch:** conceptualization, investigation, writing – review and editing, project administration, funding acquisition. **Helen Watson:** conceptualization, project administration, writing – review and editing, investigation. **Stein Rune Karlsen:** investigation, writing – review and editing, project administration, funding acquisition, conceptualization. **Benoit O. L. Demars:** conceptualization, investigation, writing – review and editing, project administration, funding acquisition, formal analysis.

Acknowledgements

We thank Finnmarkseiendommen (FeFo) and Solveig Boine Nikkinen at Mareveadji for permission to do the soil survey. We thank E. Stutter for field assistance, S. Trojahn, G. Martin for analytical assistance and A. Lilly for soil classification and for comments on the manuscript. We thank B. Johansen for the classification of the vegetation map. We appreciate and fondly remember the input of our late colleague Dr. Barry Thornton for early discussions on the project.

Conflicts of Interest

The authors declare no conflicts of interest.

Data Availability Statement

All data required to reproduce the analyses in this paper are given open access in: Stutter et al. (2025). Soil description and nutrient chemistry data from the subarctic River Tana catchment (Finmark, Norway) collected as part of the project QUANTOM. Figshare. Dataset. <https://doi.org/10.6084/m9.figshare.28696835.v1>.

References

- Abril, G., and A. V. Borges. 2019. “Ideas and Perspectives: Carbon Leaks From Flooded Land: Do We Need to Replumb the Inland Water Active Pipe?” *Biogeosciences* 16: 769–784 148.
- Aitkenhead, J. A., D. Hope, and M. Billett. 1999. “The Relationship Between Dissolved Organic Carbon in Stream Water and Soil Organic

- Carbon Pools at Different Spatial Scales." *Hydrological Processes* 13: 1289–1302.
- Alekseev, I., and E. Abakumov. 2022. "Soil Organic Carbon Stocks and Stability of Organic Matter in Permafrost-Affected Soils of Yamal Region, Russian Arctic." *Geoderma Regional* 28: e00454.
- Alekseev, I., T. Alekseev, V. Ostromov, et al. 2003. "Mineral Transformations of Permafrost Affected Soils." *Soil Science Society of America Journal* 67: 596–605.
- Arnoldussen, A. H. 1999. "Soil Survey in Norway." In *European Soil Bureau Research*. Report No.6, EUR 18991 EN, edited by Soil Resources of Europe, P. Bullock, R. J. A. Jones, and L. Montanarella, 123–128. Office for Official Publications of the European Communities.
- Bartlett, J., G. M. Rusch, M. O. Kykjeeide, H. Sandvik, and J. Nordén. 2020. *Carbon Storage in Norwegian Ecosystems (Revised Edition)*. Karbonlagring i Norske økosystemer (Revidert Utgave). NINA report 1774b. Norwegian Institute for Nature Research.
- Batjes, N. H. 2002. "Carbon and Nitrogen Stocks in the Soils of Central and Eastern Europe." *Soil Use and Management* 18: 324–329.
- Berggren, M., F. Guillemette, M. Bieroza, et al. 2022. "Unified Understanding of Intrinsic and Extrinsic Controls of Dissolved Organic Carbon Reactivity in Aquatic Ecosystems." *Ecology* 13: e3763. <https://doi.org/10.1002/ecy.3763>.
- Boorman, D. B., J. M. Hollis, and A. Lilly. 1995. *Hydrology of Soil Types: A Hydrologically-Based Classification of the Soils of the United Kingdom*. Report 126. Institute of Hydrology.
- Broll, G., F.-K. Holtmeier, K. Anschlag, H.-J. Braukmann, S. Wald, and B. Drees. 2007. "Landscape Mosaic in the Treeline Ecotone on Mt Rodjanoaivi, Subarctic Finland." *Fennia* 185: 89–105.
- Covino, T. 2017. "Hydrologic Connectivity as a Framework for Understanding Biogeochemical Flux Through Watersheds and Along Fluvial Networks." *Geomorphology* 277: 133–144. <https://doi.org/10.1016/j.geomorph.2016.09.030>.
- Cransac, L. 2023. "Mechanisms Driving Stream Organic Carbon Mass Balance at Catchment Scale in Arctic Regions: Tana Catchment, Norway." ENGEES Diploma in Luxembourg, Norwegian Institute for Water Research.
- de Brogniez, D., C. Ballabio, A. Stevens, R. J. A. Jones, L. Montanarella, and B. van Wesemael. 2015. "A Map of the Topsoil Organic Carbon Content of Europe Generated by a Generalized Additive Model." *European Journal of Soil Science* 66: 121–134. <https://doi.org/10.1111/ejss.12193>.
- Devos, C. C., M. Ohlson, E. Næsset, and O. M. Bollandsås. 2022. "Soil Carbon Stocks in Forest-Tundra Ecotones Along a 500 km Latitudinal Gradient in Northern Norway." *Nature Scientific Reports* 12: 13358. <https://doi.org/10.1038/s41598-022-17409-3>.
- Drusch, M., U. Del Bello, S. Carlier, et al. 2012. "Sentinel-2: ESA's Optical High-Resolution Mission for GMES Operational Services." *Remote Sensing of Environment* 120: 25–36. <https://doi.org/10.1016/j.rse.2011.11.026>.
- European Space Agency. 2024. "Copernicus DEM – GLO-30." <https://doi.org/10.5270/ESA-c5d3d65>.
- Farmer, V. C., J. D. Russell, and B. F. L. Smith. 1983. "Extraction of Inorganic Forms of Translocated Al, Fe and Si From a Podzol Bs Horizon." *Journal of Soil Science* 34: 571–576.
- Filius, J. D., D. G. Lumsdon, J. C. L. Meussen, T. Hiemstra, and W. H. van Riemsdijk. 2000. "Adsorption of Fulvic Acid on Goethite." *Geochimica et Cosmochimica Acta* 64: 51–60.
- Frey, K. E., J. W. McClelland, R. M. Holmes, and L. C. Smith. 2007. "Impacts of Climate Warming and Permafrost Thaw on the Riverine Transport of Nitrogen and Phosphorus to the Kara Sea." *Journal of Geophysical Research* 112: G04S58. <https://doi.org/10.1029/2006JG000369>.
- Gomez-Velez, J., J. Harvey, M. Cardenas, et al. 2015. "Denitrification in the Mississippi River Network Controlled by Flow Through River Bedforms." *Nature Geoscience* 8: 941–945. <https://doi.org/10.1038/geo2567>.
- Harms, T. K., and S. M. Ludwig. 2016. "Retention and Removal of Nitrogen and Phosphorus in Saturated Soils of Arctic Hillslopes." *Biogeochemistry* 127: 291–304. <https://doi.org/10.1007/s10533-016-0181-0>.
- IUSS Working Group WRB. 2022. *World Reference Base for Soil Resources. International Soil Classification System for Naming Soils and Creating Legends for Soil Maps*. 4th ed. International Union of Soil Sciences (IUSS).
- Jansen, B., K. Kalbitz, and W. H. McDowell. 2014. "Dissolved Organic Matter: Linking Soils and Aquatic Systems." *Vadose Zone Journal* 13: 1–4. <https://doi.org/10.2136/vzj2014.05.0051>.
- Johansen, B., and S. R. Karlsen. 2005. "Monitoring Vegetation Changes on Finnmarksvidda, Northern Norway, Using Landsat MSS and Landsat TM/ETM Plus Satellite Images." *Phytocoenologia* 35: 969–984. <https://doi.org/10.1127/0340-269X/2005/0035-0969>.
- Karlsen, S. R., D. Trosten, and B. Johansen. 2023. *Finnmarksvidda – Status 2023. Kartlegging og Overvåkning av Reinbeiter*. NORCE Report 13/23. NORCE Norwegian Research Centre.
- Karlsen, S. R., H. Tømmervik, B. Johansen, and J. Å. Riseth. 2017. "Future Forest Distribution on Finnmarksvidda, North Norway." *Climate Research* 73: 125–133. <https://doi.org/10.3354/cr01459>.
- Kaste, Ø., C. B. Gundersen, J. Sample, et al. 2024. "The Norwegian River Monitoring Programme 2023 – Water Quality Status and Trends." *Elveovervåkningsprogrammet 2023 – vannkvalitetstilstand og trender*. NIVA report 8006–2024. Accessed April 2025. <https://www.miljodirektoratet.no/publikasjoner/2024/oktober-2024/the-norwegian-river-monitoring-programme-2023--water-quality-status-and-trends/>.
- Kawahigashi, M., K. Kaiser, A. Rodionov, and G. Guggenberger. 2006. "Sorption of Dissolved Organic Matter by Mineral Soils of the Siberian Forest Tundra." *Global Change Biology* 12: 1868–1877.
- Kjær, S. T., S. Westermann, N. Nedkvitne, and P. Dörsch. 2024. "Carbon Degradation and Mobilisation Potentials of Thawing Permafrost Peatlands in Northern Norway Inferred From Laboratory Incubations." *Biogeosciences* 21: 4723–4737. <https://doi.org/10.5194/bg-21-4723-2024>.
- Kjellman, S. E., P. E. Axelsson, B. Etzelmüller, S. Westermann, and A. B. K. Sannel. 2018. "Holocene Development of Subarctic Permafrost Peatlands in Finnmark, Northern Norway." *Holocene* 28: 1855–1869.
- Krause, S., J. Lewandowski, N. B. Grimm, et al. 2017. "Ecohydrological Interfaces as Hot Spots of Ecosystem Processes." *Water Resources Research* 53: 6359–6376. <https://doi.org/10.1002/2016WR019516>.
- Laudon, H., and R. A. Sponseller. 2018. "How Landscape Organization and Scale Shape Catchment Hydrology and Biogeochemistry: Insights From a Long-Term Catchment Study." *WIREs Water* 5: e1265. <https://doi.org/10.1002/wat2.1265>.
- Lidman, F., Å. Boily, H. Laudon, and S. J. Köhler. 2017. "From Soil Water to Surface Water – How the Riparian Zone Controls the Transport of Major and Trace Elements From a Boreal Forest to a Stream." *Biogeosciences* 14: 3001–3014.
- Lim, A. G., S. V. Loiko, and O. S. Pokrovsky. 2022. "Sizeable Pools of Labile Organic Carbon in Peat and Mineral Soils of Permafrost Peatlands, Western Siberia." *Geoderma* 409: 115601. <https://doi.org/10.1016/j.geoderma.2021.115601>.
- Liu, S., T. Maavara, C. B. Brinkerhoff, and P. A. Raymond. 2022. "Global Controls on DOC Reaction Versus Export in Watersheds: A Damköhler Number Analysis." *Global Biogeochemical Cycles* 36: e2021GB007278. <https://doi.org/10.1029/2021GB007278>.

- Miner, K. R., J. D'Andrilli, R. Mackelprang, et al. 2021. "Emergent Biogeochemical Risks From Arctic Permafrost Degradation." *Nature Climate Change* 11, no. 10: 809–819.
- Mueller, C. W., J. Rethemeyer, J. Kao-Kniffin, S. Löppmann, K. M. Hinkel, and J. G. Bockheim. 2015. "Large Amounts of Labile Organic Carbon in Permafrost Soils of Northern Alaska." *Global Change Biology* 21: 2804–2817.
- NSDB. 2022. "National Soil Database for Canada: National Pedon Database." Accessed December 16, 2024. <https://sis.agr.gc.ca/cansis/nsdb/npdb/index.html>.
- Obu, J., H. Lantuit, I. Myers-Smith, B. Heim, J. Wolter, and M. Fritz. 2017. "Effect of Terrain Characteristics on Soil Organic Carbon and Total Nitrogen Stocks in Soils of Herschel Island, Western Canadian Arctic." *Permafrost and Periglacial Processes* 28: 92–107.
- Ola, A., D. Fortier, S. Coulombe, J. Comte, and F. Domine. 2022. "The Distribution of Soil Carbon and Nitrogen Stocks Among Dominant Geomorphological Terrain Units in Qarliktuvik Valley, Bylot Island, Arctic Canada. Journal of Geophysical Research." *Biogeosciences* 127: e2021JG006750. <https://doi.org/10.1029/2021JG006750>.
- Ping, C.-L., G. J. Michaelson, M. T. Jorgenson, et al. 2008. "High Stocks of Soil Organic Carbon in North American Arctic Region." *Nature Geoscience* 1: 615–619. <https://doi.org/10.1038/ngeo284>.
- Ploum, S. W., J. A. Leach, H. Laudon, and L. Kuglerová. 2021. "Groundwater, Soil, and Vegetation Interactions at Discrete Riparian Inflow Points (DRIPs) and Implications for Boreal Streams." *Frontiers in Water* 3: 669007. <https://doi.org/10.3389/frwa.2021.669007>.
- Prowse, T., A. Bring, J. Mård, and E. Carmack. 2015. "Arctic Freshwater Synthesis: Introduction." *Journal of Geophysical Research: Biogeosciences* 120, no. 11: 2121–2131. <https://doi.org/10.1002/2015JG003127>.
- QGIS Development Team. 2024. *QGIS Geographic Information System, Version 3.34.12*. Open-Source Geospatial Foundation Project.
- Ryan, K. A., V. A. Garayburu-Caruso, B. C. Crump, et al. 2024. "Riverine Dissolved Organic Matter Transformations Increase With Watershed Area, Water Residence Time, and Damköhler Numbers in Nested Watersheds." *Biogeochemistry* 167: 1203–1224. <https://doi.org/10.1007/s10533-024-01169-5>.
- Scheider, M. K., F. Brunner, J. M. Hollis, and C. Stamm. 2007. "Towards a hydrological classification of European soils: Preliminary test of its predictive power for the base flow index using river discharge data." *Hydrology and Earth System Sciences Discussion* 4: 831–861.
- Shogren, A. J., J. P. Zarnetske, B. W. Abbott, et al. 2019. "Revealing Biogeochemical Signatures of Arctic Landscapes With River Chemistry." *Nature Scientific Reports* 9: 12894. <https://doi.org/10.1038/s41598-019-49296-6>.
- Smith, B. F. L., and D. C. Bain. 1982. "A Sodium Hydroxide Fusion Method for the Determination of Total Phosphate in Soils." *Communications in Soil Science and Plant Analysis* 13: 185–190.
- Soil Survey Staff. 1999. "Soil Taxonomy: A Basic System of Soil Classification for Making and Interpreting Soil Surveys." In *Natural Resources Conservation Service*, 2nd ed., 436. U.S. Department of Agriculture Handbook.
- Stutter, M., L. Jackson-Blake, A. Lilly, et al. 2025. "Soil Description and Nutrient Chemistry Data From the Subarctic River Tana Catchment (Finmark, Norway) Collected as Part of the Project QUANTOM." Figshare. Dataset. <https://doi.org/10.6084/m9.figshare.28696835.v1>.
- Stutter, M., N. J. Baggaley, J. Davies, et al. 2023. "The Riparian Reactive Interface: A Climate-Sensitive Gatekeeper of Global Nutrient Cycles." *Frontiers in Environmental Science* 11: 1213175. <https://doi.org/10.3389/fenvs.2023.1213175>.
- Uhlig, C., T. E. Sveistrup, and I. Schjelderup. 2004. "Impacts of Reindeer Grazing on Soil Properties on Finnmarksvidda, Northern Norway." *Rangifer* 24, no. 4: 83–91. <https://doi.org/10.7557/2.24.4.1726>.

Supporting Information

Additional supporting information can be found online in the Supporting Information section. **Table S1a:** Cær, lower (1 m distance from stream) soil plots. **Table S1b:** Cær, middle (15 m distance from stream) soil plots. **Table S1c:** Cær, upper (25 m distance from stream) soil plots. **Table S2a:** Mar, lower (0.5 m distance from stream) soil plots. **Table S2b:** Mar, upper (10 m distance from stream) soil plots. **Table S3a:** Ski, lower (1 m distance from stream) soil plots. **Table S3b:** Ski, middle (15 m distance from stream) soil plots. **Table S3c:** Ski, upper (30 m distance from stream) soil plots. **Table S4a:** Dar, lower (1 m distance from stream) soil plots. **Table S4b:** Dar, middle (15 m distance from stream) soil plots. **Table S4c:** Dar, upper (25 m distance from stream) soil plots. **Table S5:** Details of soil WRB and hydrology of soil types (HOST) classifications, with the dominant conceptual models depicted. **Table S6:** REML testing data of factors: Landscape position ($n=3$), Soil horizon groups ($n=3$), Sites ($n=3$), Horizon \times Position on \log_{10} transformed data (except soil pH) with F-statistic values. Stated p values refer to REML outputs, but bold font denotes results presented as significant following Bonferroni correction (see methods, cut-off $p < 0.002$). **Table S7:** ANOVA General Linear Model Tukey comparison tests for factors: Landscape position ($n=3$), Soil horizon groups ($n=3$), Sites ($n=3$), taken from 3-way ANOVA model with interactions on \log_{10} transformed data (except soil pH). Different letters denote Tukey significant differences ($p < 0.002$ Bonferroni correction onto the 95% threshold) and bold font highlights where differences were significant. Values are data means (non-transformed values). **Figure S1:** Soil bulk density (BD) relationship with determined soil carbon concentration derived from sampled soil cores ($n=85$) and used to derived model estimates of BD for 51 horizons that could not be sampled in cores due to stone contents. **Figure S2:** Confidence interval (99.8%) plots for the Tukey post-ANOVA differences for solid phase macronutrient analyses. Position (left column of graphs) groups are: 1, lower; 2, mid; 3, upper; horizons (mid column) groups are: 1, organic topsoil; 2, mineral topsoil; 3, subsoil; and site (right column) are 1, Cær; 2, Mar; 3, Ski; 4, Dar. Determinants are in same order as Table S6 (zoom in on electronic file for details). **Figure S3:** Confidence interval (99.8%) plots for the Tukey post-ANOVA differences for soil geochemical properties. Position (left column of graphs) groups are: 1, lower; 2, mid; 3, upper; horizons (mid column) groups are: 1, organic topsoil; 2, mineral topsoil; 3, subsoil; and site (right column) are 1, Cær; 2, Mar; 3, Ski; 4, Dar. Determinants are in same order as Table S6 (zoom in on electronic file for details). **Figure S4:** Confidence interval (99.8%) plots for the Tukey post-ANOVA differences for water extractable nutrients. Position (left column of graphs) groups are: 1, lower; 2, mid; 3, upper; horizons (mid column) groups are: 1, organic topsoil; 2, mineral topsoil; 3, subsoil; and site (right column) are 1, Cær; 2, Mar; 3, Ski; 4, Dar. Determinants are in same order as Table S6 (zoom in on electronic file for details).